HHS Public Access

Author manuscript

Nat Commun. Author manuscript; available in PMC 2015 October 13.

Published in final edited form as:

Nat Commun. ; 6: 6763. doi:10.1038/ncomms7763.

A fungal protease allergen provokes airway hyperresponsiveness in asthma

Nariman A. Balenga[1], **Michael Klichinsky**[2], **Zhihui Xie**[1], **Eunice C. Chan**[1], **Ming Zhao**[3], **Joseph Jude**[2], **Michel Laviolette**[4], **Reynold A. Panettieri Jr**[2], and **Kirk M. Druey**[1,*]

[1]Molecular Signal Transduction Section, Laboratory of Allergic Diseases, NIAID/NIH, 50 South Drive Room 4154, Bethesda, MD 20892-8305

[2]Pulmonary, Allergy and Critical Care Division, Airways Biology Initiative, University of Pennsylvania, 125 South 31st St, Philadelphia, PA 19104-3413

[3]Protein Chemistry, Research Technologies Branch, Twinbrook I, 5640 Fishers Lane Room 1012 NIAID/NIH, Rockville, MD 20852-1737

[4]Institut universitaire de cardiologie et pneumologie de Québec (Laval University) Département multidisciplinaire de pneumologie et de chirurgie thoracique de l'IUCPQ, L35312725, chemin Sainte-Foy, Québec Canada G1V 4G5

Abstract

Asthma, a common disorder that affects more than 250 million people worldwide, is defined by exaggerated bronchoconstriction to inflammatory mediators including acetylcholine, bradykinin, and histamine—also termed airway hyper-responsiveness Nearly 10% of people with asthma have severe, treatment-resistant disease, which is frequently associated with IgE sensitization to ubiquitous fungi, typically *Aspergillus fumigatus*. Here we show that a major *Aspergillus fumigatus* allergen, *Asp f13*, which is a serine protease, alkaline protease 1 (Alp 1), promotes airway hyper-responsiveness by infiltrating the bronchial submucosa and disrupting airway smooth muscle cell-extracellular matrix interactions. Alp 1-mediated extracellular matrix degradation evokes pathophysiological RhoA-dependent Ca^{2+} sensitivity and bronchoconstriction. These findings support a pathogenic mechanism in asthma and other lung diseases associated with epithelial barrier impairment, whereby airway smooth muscle cells respond directly to inhaled environmental allergens to generate airway hyper-responsiveness.

*To whom correspondence should be addressed at: 50 South Drive Room 4154, Bethesda, MD 20892-8305; ph: 301-435-8875, fax: 301-451-1616; kdruey@niaid.nih.gov.

Author Contributions

N.A.B. and K.M.D. designed the project and wrote the manuscript. N.A.B. designed and performed most of the experiments. M.K. performed experiments shown in Fig. 3a–h and 6a–b. J.J. contributed experiments to Figs. 1b–e, 6h, and 7b. M.Z. performed experiments shown in Fig. 1a,Supplementary Figs. 3a–b and 4. Z.X. performed experiments shown in Fig. 4c and 5e. E.C.C. contributed to experiments shown in Figs. 2a, 6h, 7d, f. R.A.P. designed experiments, analyzed data, provided critical cell lines, and edited the manuscript. M.L. provided clinical samples and data, assisted in interpretation of data in Table 1 and Fig. 8, and edited the manuscript.

Competing financial interests

The authors declare no competing financial interests.

In asthma, chronic lung inflammation due to the immune response to inhaled allergens leads to desquamation of the respiratory epithelium, increased bronchial smooth muscle mass, and mucous gland hypertrophy[1,2] However, the mechanisms by which such airway "remodeling" brings about enhanced contraction of airway smooth muscle (ASM) cells to pro-contractile ligands are poorly understood[3]. Intraperitoneal immunization of mice with a diverse array of allergens including ovalbumin (OVA), house dust mite (HDM), or *Af* followed by respiratory mucosal challenge induces what is termed "allergic sensitization": expansion of allergen-specific T helper type 2 (T_H2) cells, synthesis of allergen-specific IgE, and production of cytokines in lung including IL-4, IL-5, and IL-13. These events result in allergic inflammation including goblet cell metaplasia, increased mucous production, leukocyte infiltration (predominantly eosinophils), and collagen deposition in the bronchial submucosa[4–7].

Protease activity is a common and important feature of many allergens capable of inducing asthma. A secreted protease of *Aspergillus oryzae* (*Ao*) was shown to elicit T_H2 immunity and allergic inflammation in mice through proteolytic cleavage of fibrinogen. Fibrinogen cleavage products can act as Toll-like receptor 4 (TLR4) ligands on respiratory epithelial cells, innate lymphoid cells, and macrophages to elicit cytokine production and upregulation of mucin genes that promote the asthma phenotype[8]. Serine protease allergens can both activate and impair respiratory epithelial functions. An alkaline serine protease from the allergenic fungus *Penicillium citrinum* (*Pen c13*) induced proinflammatory cytokine release in airway epithelial cells through activation of coagulation factor II (thrombin) receptor and coagulation factor II-like receptor 2 [F2R and F2RL1, previously known as protease activated receptors (PAR) 1 and 2][9]. Both *Pen c 13* and a serine protease component of the ubiquitous mold *Alternaria alternata* induce respiratory epithelial barrier dysfunction through altered cell-cell junctions and actin cytoskeletal rearrangements[10,11].

Induction of allergic sensitization and airway hyper-responsiveness (AHR) in mice by allergens generally requires priming with both the allergen and an adjuvant at sites distant from the lung. However, short-term respiratory mucosal exposure of mice to protease-containing allergens such as *Af* or *Ao* may evoke AHR without prior remote priming with allergen and adjuvant[12]. Inhalation of proteolytically active *Ao*, but not its protease-inactive counterpart, elicited nearly equivalent AHR in the presence or absence of ovalbumin (OVA), which did not correlate strictly with the magnitude of allergic inflammatory response (IgE response, airway eosinophilia). Likewise, the purified, secreted *Af* protease, which itself is poorly immunogenic[13], induced AHR in the presence of OVA despite recruiting markedly fewer airway eosinophils to the lung than OVA plus crude *Af* allergen. These results suggest that proteolytic activity of certain allergens, while not sufficient to elicit AHR in the absence of lung inflammation, nonetheless contribute to AHR through mechanisms independent of allergic sensitization.

Whether allergens have a direct and pathogenic impact on ASM contraction in asthma has not been explored. Here, we investigate the hypothesis that lung epithelial destruction associated with asthma permits penetrance of allergen components into the bronchial submucosa to promote ASM contraction. We detect an *Af*-derived protease (Alp 1) in the bronchial smooth muscle layer of human subjects with asthma and allergen-challenged mice

but not in control subjects or naïve mice, and we provide a potential mechanism by which Alp 1 induces a pro-contractile phenotype of ASM cells.

Results

Af protease activity promotes airway hyper-responsiveness

Proteolytic enzymes secreted by *Af* cause epithelial desquamation and have an integral function in tissue invasiveness[14,15]. We found that a commercially available and clinically used *Af* extract had readily detectable protease activity, which was abolished by heat inactivation or preincubation with inhibitors of serine proteases (PMSF or antipain), but not cysteine proteases (E-64) (Fig. 1a). To determine the relative importance of *Af* protease activity for the induction of AHR, we sensitized and challenged mice with either native or heat-inactivated (HI)-*Af* allergen extracts and measured total lung resistance (R_L) in anesthetized mice following methacholine inhalation. As expected, mice challenged with untreated *Af* had significantly increased R_L compared to naïve mice (Fig. 1b). Mice challenged with HI-*Af* had significantly reduced R_L values compared to mice that received untreated *Af*. However, native or heat-inactivated *Af* induced comparable sensitization, as evidenced by equivalent peribronchial inflammation, goblet cell metaplasia (Fig. 1c), and total cell counts in bronchoalveolar lavage fluid (Fig. 1d), although the composition of BAL fluid differed modestly between the two groups. Challenge with HI-*Af* elicited slightly fewer airway eosinophils and a greater influx of neutrophils than did challenge with untreated *Af* (Fig. 1e). These results suggest that *Af* protease activity also contributes to AHR through mechanisms distinct from the inflammatory response.

Af induces lung slice airway contraction

To determine whether *Af* could elicit bronchoconstriction without prior allergic sensitization, we pretreated precision-cut lung slices (PCLS) extracted from lungs of naïve mice with *Af* extracts for twenty-four hours and visualized airway contraction in response to carbachol (an acetylcholine analog similar to methacholine). Compared to PCLS incubated with vehicle alone, lung slices pretreated with *Af* had spontaneously narrowed airways at baseline (Fig. 2a) and displayed a dose-dependent increase in carbachol-mediated bronchoconstriction [E_{max}: vehicle = 31.99 ± 2; *Af* (5 μg ml^{-1}) = 53.06 ± 3.5; *Af* (10 μg ml^{-1}) = 66.64 ± 3.7; $P < 0.0001$; EC_{50} unchanged] (Fig. 2b). In contrast, vehicle- and *Af*-pretreated PCLS had equivalent contraction in response to KCl, which depolarizes cell membranes through a voltage-gated Ca^{2+} channel[16,17] (Fig. 2c). Together, these findings indicated that *Af* specifically and independently augments G-protein-coupled receptor (GPCR)-mediated bronchoconstriction in the absence of prior allergen sensitization and challenge.

Af enhances Ca^{2+} mobilization in airway smooth muscle cells

Our results suggested that *Af* promotes AHR by augmenting ASM contraction partially through inflammation-independent mechanisms. Agonist stimulation of GPCRs induces bronchoconstriction initially by increasing cytosolic Ca^{2+} levels[18,19]. To determine whether *Af* affected GPCR-evoked Ca^{2+} signaling, we incubated cultured human ASM cells (HASM) with *Af* extract for twenty-four hours prior to quantification of cytosolic Ca^{2+} by fluorescence microscopy. *Af* pretreatment led to an increase in basal cytosolic Ca^{2+} in a

concentration-dependent manner (Fig. 3a) and significantly enhanced intracellular Ca^{2+} flux in response to GPCR ligands bradykinin or histamine compared to vehicle-treated cells (Fig. 3b–e). In contrast, vehicle and *Af*-treated HASM displayed similar responses to ionomycin (Fig. 3f), which increase cytosolic Ca^{2+} through receptor-independent mechanisms. GPCR-mediated Ca^{2+} mobilization is dependent upon PLCβ-mediated generation of inositol 1, 4, 5-trisphosphate (Ins_{P3}), which in turn stimulates Ins_{P3} receptors on sarcoplasmic reticulum to release Ca^{2+} into the cytosol. Accordingly, we observed increased amounts of bradykinin-evoked Ins_{P1} (a stable metabolite of Ins_{P3}) in *Af*-pretreated HASM cells compared to controls (Fig 3g).

Addition of *Af* extract to HASM immediately prior to measurement of Ca^{2+} concentrations (i.e. without prolonged preincubation) failed to induce any Ca^{2+} mobilization, and simultaneous stimulation of cells with *Af* extract and bradykinin did not potentiate Ca^{2+} signaling induced by bradykinin alone (Fig. 3h). These results suggested that *Af* does not activate Ca^{2+} signaling through a protease-activated receptor, such as F2R or F2LR1. In support of this hypothesis, we found that 24-hour pretreatment of ASM with *Af* actually abolished responses to thrombin and resulted in profoundly diminished levels of F2R at the plasma membrane (Fig. 3i–j). Thus, chronic exposure of HASM cells to *Af* may potentiate GPCR-evoked Ca^{2+} spikes in a receptor-independent manner.

Af degrades extracellular matrix

Exposure of ASM cells to *Af* could also affect expression of receptors or elements of the excitation-contraction signaling pathway that elicit bronchoconstriction. We failed to detect increased expression of contraction-inducing receptors or intracellular contractile proteins in HASM following *Af* treatment (Supplementary Figure 1a). However, incubation with *Af* induced profound changes in HASM cell morphology, including elongation and detachment, disassembly of vinculin-rich focal adhesions (adhesomes), reduced actin stress fibers (Fig. 4a–b), and haptotaxis (Supplementary Movies 1–2), without altering vinculin expression (Supplementary Figure 1b) or eliciting changes in cell viability, apoptosis, or proliferation (Supplementary Figure 2). These results suggested that *Af* perturbs integrin-mediated extracellular matrix (ECM) attachments of HASM.

ECM activation of membrane bound integrins elicits autophosphorylation of focal adhesion kinase (FAK), actin polymerization, and assembly of a signalosome of cytoskeletal proteins including vinculin, paxillin, and α-actinin, which are essential for actomyosin crossbridging and force generation[20,21]_ENREF_17. Surprisingly, however, deficiency of α9β1 integrin in ASM by conditional genetic deletion of α9 (*Itga9*) in mice resulted in spontaneous AHR[22]. We observed markedly reduced surface expression and increased cytosolic localization of α9 integrin in *Af*-treated cells compared to controls by immunofluorescent staining (Fig. 4c). Heat inactivation or pre-incubation of *Af* extract with a serine protease inhibitor prior to addition to HASM cells prevented *Af*-induced morphological change and detachment (Fig. 4a) as did pre-coating plates with exogenous ECM proteins including collagen I and fibronectin (Fig. 4d–e). Together, these results indicated that one or more serine proteases present in *Af* allergen extracts might digest ECM components to disrupt integrin-mediated attachments in ASM cells.

A prior study demonstrated that a serine protease purified from *Af* culture supernatants degraded multiple ECM proteins, including elastin, collagen types I-III, and fibronectin23. Hence, we found that the *Af* allergen extract used here reduced the collagen content of HASM cells in culture (Fig. 5a) and of PCLS (Fig. 5b) and digested several purified ECM components (Fig. 5c–d). We also determined whether exposure of HASM cells to *Af* induced production of matrix metalloproteinases (MMPs) or tissue inhibitor of metalloproteinases (TIMPs) that are expressed by HASM and could affect ECM composition[24,25]. *Af* treatment of HASM increased secretion of MMP1 and MMP3 compared to vehicle treatment, but not any of the others tested including MMP2, 8, 9, 10 or TIMPs 1, 2 and 4 (Fig. 5e).

Notably, we detected substantially less protease activity in extracts of another common allergen, house dust mite (HDM), than in *Af* solutions with equivalent protein concentrations. HDM extract induced morphological changes and detachment of HASM cells only at much higher concentrations than did active *Af*, and these effects were abolished by addition of cysteine protease inhibitors (Supplementary Figure 3).

Af modifies Ca^{2+} signaling in airway smooth muscle cells

Integrin-mediated ECM interactions and the formation of focal adhesion plaques may affect the metabolism of membrane phospholipids that mediate GPCR-induced Ca^{2+} spikes. Deletion of integrin α9 in mouse smooth muscle increased production of phosphatidylinositol 4,5-bisphosphate ($Ins(4,5)_{P2}$ or PIP2), which is the principal substrate of PLCβ[22]. I ntegrin activation and FAK phosphorylation also activate Rho GTPase activating protein (p190RhoGAP), a negative regulator of RhoA activity. RhoA-associated coiled-coil forming kinase (ROCK) in turn activates phosphatidylinositol 4-phosphate 5-kinases (PIP5K), a group of enzymes that catalyze the production of PIP2. We detected increased Ins_{P3} in HASM cells incubated with *Af* (Fig. 3g). Addition of purified ECM components (collagen I) to HASM cultures significantly reduced *Af*-evoked augmentation of Ca^{2+} transients (Fig. 6a–c), suggesting that dysregulation of cell-ECM contacts by *Af* protease activity increased GPCR-induced Ins_{P3} production. Incubation of HASM with *Af* abolished FAK autophosphorylation (Fig. 6d) and increased both basal and bradykinin-induced RhoA activation compared to vehicle-treated cells (Fig. 6e–f). Consequently, cellular PIP2 levels were increased in *Af*-treated cells compared to controls (Fig. 6g). Thus, increased availability of PIP2 substrate may contribute to the enhanced agonist-induced Ins_{P3} production and Ca^{2+} mobilization we observed following *Af* treatment.

ROCK also promotes ASM contraction by inhibiting myosin light chain phosphatase through phosphorylation of its MYPT1 subunit[18]. As a result, myosin light chain (MLC) phosphorylation is enhanced, which facilitates actomyosin crossbridging and ASM contraction. *Af* treatment of HASM cells increased both ROCK activity (MYPT1 phosphorylation) and the basal phosphorylation of MLC (Fig. 6h). Finally, pretreatment of PCLS with the ROCK inhibitor Y27632 reversed the enhanced carbachol-evoked contraction of airways in PCLS treated with *Af* but had little effect on contraction in vehicle-treated slices (Fig. 6i). This result suggests that *Af* mediates bronchoconstriction predominantly by augmenting ROCK-mediated Ca^{2+} sensitivity in ASM cells.

Alp 1 mediates *Af*-evoked bronchoconstriction

We used ion exchange chromatography and gel filtration to identify serine protease(s) responsible for the hypercontractile ASM phenotype (Supplementary Figure 4). Mass spectrometric analysis indicated that Alp 1 was the sole serine protease present in active *Af* extract fractions. By estimates of recovery from purification procedures and by using quantitative immunoblotting with specific polyclonal Alp 1 antisera and purified standards, we determined that Alp 1 accounted for approximately 1% of the total protein in crude *Af* extracts (10–60 μg ml^{-1}) (Supplementary Figure 5a–b), indicating that Alp 1 concentrations in *Af* used for *in vitro* assays were roughly 0.001-0.1 μg ml^{-1} (see Figure 2–Figure 6). However, we estimate that the purified protein had only 10% of the protease activity of crude extracts containing equivalent concentrations of Alp 1, indicating substantial loss of protease activity during purification (Supplementary Fig. 5c). Treatment of HASM cells with purified Alp 1 induced cell detachment and elongation, and both outcomes were dependent on Alp 1 serine protease activity (Fig. 7a). Using the much more sensitive Ca^{2+} assay, we found that incubation of HASM with purified Alp 1 at concentrations as low as 0.001 μg ml^{-1} significantly enhanced bradykinin-evoked Ca^{2+} spikes (Fig. 7b). We determined whether *Af* protease activity was required for augmentation of HASM responses to contractile agonists and bronchoconstriction using heat inactivated extracts. HI *Af* did not enhance agonist-evoked Ca^{2+} mobilization (Fig. 7b) or MYPT1 and MLC2 phosphorylation (Fig. 7c), nor did it significantly augment carbachol-evoked bronchoconstriction of airways in PCLS (Fig. 7d). By contrast, treatment of HASM cells with purified Alp 1 substantially increased MYPT1 and MLC phosphorylation compared to vehicle alone (Fig. 7e), and pre-treatment of PCLS with purified Alp 1 at concentrations as low as 0.1 μg ml^{-1} significantly increased carbachol-mediated airway contraction in PCLS compared to controls (Fig. 7f). Together, these results suggest that Alp 1 protease mediates the bronchoconstriction induced by *Aspergillus fumigatus* crude allergenic extracts.

Alp 1 is present in human and murine bronchi

To determine the extent to which Alp 1 reaches the airway submucosa to induce AHR *in vivo*, we performed immunostaining on mouse and human lung sections with anti-Alp 1 antisera. We sensitized mice intraperitoneally with *Af* followed by repeated intranasal challenge with *Af* extracts. We detected Alp 1 in bronchial smooth muscle of mice sensitized and challenged with *Af*, but not in naïve mice, or in animals simply inoculated intranasally with *Af* for four hours or overnight prior to lung harvest in the absence of prior sensitization (Fig. 8a and Supplementary Figure 5d). We also detected Alp 1 in the lung tissue (Fig. 8b) and BAL fluid (Fig. 8c) of *Af*-sensitized and challenged mice by immunoblotting but not in naïve mice. Based on quantitative immunoblotting, Alp 1 concentrations in BAL fluid were approximately 0.005 μg ml^{-1} (Supplementary Fig. 5b), suggesting that we used physiologically relevant concentrations for *in vitro* assays. Collectively, these results demonstrated that both the allergic inflammatory response to *Af* and allergen protease activity seemed to be required for Alp 1 dissemination in the bronchial submucosa in mice.

To extend these findings to humans, we examined lung sections from control subjects or those patients with mild to moderate asthma for the presence of Alp 1. Clinical characteristics of the patient groups are summarized in Table 1. While we detected minimal

Alp 1 staining in bronchial smooth muscle bundles of lungs from healthy subjects, Alp 1 immunostaining was present in the ASM layer of lung sections from subjects with non-atopic asthma (Fig. 8d), and further elevated levels of Alp 1 immunoreactivity were observed in ASM of patients with asthma and *Af* sensitization (epicutaneous reactivity) (Fig. 8d–e). To evaluate the relationship between Alp 1 smooth muscle staining and AHR, we determined the provocative methacholine concentration that induced a 20% decrease in the forced expiratory volume in one second ($PC20_{FEV1}$) for each subject. There was a significant negative correlation between the amount of Alp 1 detected in the bronchial submucosa and the $PC20_{FEV1}$ (Fig. 8f).

Discussion

ECM composition and deposition are radically altered in both allergic and non-allergic asthma[26–28].Our results suggest a novel pathophysiological mechanism whereby inflammation associated with respiratory mucosal exposure to *Af* allergen leads to ECM degradation through direct contact between a protease component and the bronchial submucosa. The serine protease Alp 1 secreted by *Af* digested ECM components directly and stimulated MMP1 release from ASM cells.We established that Alp 1 serine protease activity present in *Af* allergen extracts enhanced Ca^{2+} sensitivity (reduced MYPT1 activity and increased MLC phosphorylation) in cultured ASM cells by disrupting integrin-dependent ASM-ECM attachments and increasing RhoA and ROCK activity. Consequently, *Af* failed to augment airway contraction in PCLS pretreated with a ROCK inhibitor, suggesting that it induced bronchoconstriction primarily through pathogenic Ca^{2+} sensitization.

Af also evoked substantial increases in the magnitude of GPCR agonist-induced Ca^{2+} transients in cultured ASM cells. We now know that intracellular Ca^{2+} concentrations fluctuate repeatedly following agonist stimulation, in the form of a series of Ca^{2+} oscillations[29]. The force of sustained airway contraction appears to correlate primarily with the persistence and frequency of these Ca^{2+} oscillations, rather than the magnitude of the Ca^{2+} spikes. However, published work has shown that while serotonin (5-HT) induced greater airway contraction of airways in PCLS than acetylcholine (ACh), 5-HT evoked a Ca^{2+} oscillation frequency that was slower than ACh in HASM cells[30]. These results suggest that the correlation between contraction and oscillation frequency depends on the agonist studied. Thus, future measurements of Ca^{2+} oscillations and elucidation of the impact of Ca^{2+} sensitivity (inhibition of MLCP) on the frequency-contraction relationship in PCLS will allow us to better determine the significance of our *in vitro* findings for bronchial contraction *in vivo*.

How ECM-integrin interactions regulate ASM contraction *in vivo* also requires further study. Serine protease (elastase)-mediated airway destruction contributes to cigarette smoke-induced airway obstruction[31]. Treatment of lung slices from naïve mice with a serine protease (human neutrophil elastase) led to significantly increased airway contraction[32]. In a separate study, intratracheal administration of elastase to guinea pigs augmented bronchoconstriction in response to inhaled acetylcholine through an unknown mechanism[33]. Although it has been argued that integrin activation by the ECM and resultant actin filament

interactions at the plasma membrane promote force generation in smooth muscle cells by increasing membrane tension and cytoskeletal rigidity[20,21], recent work has demonstrated that integrin signaling may regulate bronchial constriction in complex ways.

For example, based on their finding that loss of α9β1 integrin in mice increased ASM contraction by stimulating PIP2 generation, Chen *et al*. also demonstrated that addition of cell-permeable PIP2 (equivalent to the effect of *Af* shown here) increased carbachol-induced constriction of human airways, which was prevented by integrin blocking antibodies[22]. A separate study found that mice lacking the integrin-binding glycoprotein Milk Fat Globule-EGF factor 8 (Mfge8 or lactadherin in humans), which is secreted by ASM, had exaggerated AHR following allergen challenge despite mounting an inflammatory response that was similar to control mice[34]. Their work suggested that in a physiological setting Mfge8-integrin binding in ASM served to suppress Ca^{2+} sensitivity through decreased expression and activation of RhoA and ROCK. In another work, integrin-collagen I attachments were shown to promote switching of bovine tracheal smooth muscle cells toward a hyperproliferative and hypocontractile phenotype in a FAK-dependent manner[35]. Collectively, these observations are consistent with our results demonstrating that perturbation of ECM-integrin-FAK interactions by *Af* leads to increased RhoA and MLC activation and bronchoconstriction.

Although *Af* protease activity was required for elicitation of maximal AHR following sensitization and challenge, our results do not exclude the possibility that allergen protease activity contributes to AHR through multiple mechanisms. Previous studies demonstrated that sensitization and intranasal challenge with purified Alp 1 alone is sufficient to induce T_H2-mediated lung inflammation and AHR[36]. Simultaneous challenge with Alp 1 purified from *Af* culture supernatants and a separate recombinant *Af* allergen (*Asp f2*) induced a synergistic inflammatory response but did not further enhance AHR compared to challenge with Alp 1 alone. These results are consistent with our finding that Alp 1 has the capacity to affect AHR through inflammation-dependent and independent mechanisms. None of these studies addressed whether or not Alp 1 protease activity was required for the asthmatic phenotype and should be interpreted cautiously since both purified and recombinant Alp 1 have weak protease activity ([13] and this study). Loss of activity may occur as a result of alterations in buffer pH and/or composition during purification, protein instability, or the presence of endogenous activators or co-factors in the crude allergen extract. Finally, *Asp f13*/Alp 1 may promote inflammation through direct effects on epithelium. Alp 1 has been shown to cause epithelial barrier dysfunction, increase *Muc5ac* gene expression, and induce cytokine production (IL-6 and IL-8)[15,37–39].

Since respiratory exposure to *Af* is quite common[5], our results indicate that an additional lung insult—allergic inflammation, a respiratory irritant, or environmental exposure in the case of non-atopic disease—may be required to promote Alp 1 penetration into the bronchial smooth muscle submucosa. Several factors may account for the presence of Alp 1 (and probably other protease allergens) in the bronchial submucosa in people with asthma but not in healthy people. Recent clinical studies have demonstrated higher rates of surface airway mycosis in subjects with asthma (74%) than in controls (16%), and fungal-induced T_H2 immunity is restricted to asthma[40]. Lungs of asthmatic subjects with *Af* sensitivity (positive

skin prick test) may be more susceptible to germination of *Af* spores and have a higher burden of *Af* recoverable from sputum[41]. Airway epithelium in subjects with asthma may be more susceptible to the permeability-inducing effects of protease allergens than that of healthy controls[11]. Taken together, these results and our work suggest that chronic pulmonary inflammation and epithelial desquamation associated with asthma promote dissemination of allergens such as Alp 1 into the bronchial smooth muscle layer. We found that extracts of another perennial allergen, HDM, contained 75% less protease activity than did *Af* extract at equivalent protein concentrations and did not induce ASM detachment or morphological changes similar to those elicited by *Af*/Alp1. As prior studies have demonstrated that HDM induces proliferation and cytokine production in ASM cells, partially through activation of F2LR1[42], it is unclear whether other environmental allergens will infiltrate the bronchial submucosa and engender AHR through mechanisms equivalent to those described here.

The inverse correlation between Alp 1 staining and a parameter of AHR ($PC20_{FEV1}$) suggest that analysis of Alp 1 in the bronchial submucosa is clinically relevant. Future studies of patients with severe asthma and/or certain disease endotypes (e.g. eosinophilic *v*. neutrophilic inflammation)[43] may be necessary to determine whether Alp 1/*Asp f13* burden in ASM, or possibly in sputum, can be used as a biomarker to classify patients with fungal-associated asthma_ENREF_37. Although our anti-Alp 1 antibody did not inhibit Alp 1 protease activity or protease-induced morphological changes of HASM cells (Supplementary Figure 6), Alp 1 remains a potential therapeutic target in this subset of patients pending development of an appropriate biologic. Our findings further suggest a rationale for serine protease, ROCK, or PIP5K inhibitors for the treatment of specific asthma phenotypes.

Methods

Reagents and antibodies

Carbachol, acetylcholine, bradykinin, histamine, ionomycin, thapsigargin, bovine serum albumin (BSA), E-64, PDGF-BB, PMSF, collagen IV, fibronectin, staurosporine and Triton X-100 were purchased from Sigma. Collagen I, and III were purchased from BD Biosciences. ROCK inhibitor Y27632 was from EMD Millipore, and Collagenase D was from Roche. Methanolic Texas Red-conjugated phalloidin was obtained from Molecular Probes. Antibodies used in this study were purchased from the following sources: mouse anti-β−actin and mouse anti-vinculin (Sigma), mouse anti-GAPDH, rabbit anti-calponin, rabbit anti-SM22 and rabbit anti-B2R (Abcam), mouse anti-PLCβ (BD Biosciences), rabbit anti-ROCK1, rabbit anti-FAK, rabbit anti-$pFAK^{Y397}$ (Cell Signaling), mouse anti-Rac1 and mouse anti-RhoA (Millipore).

Immunoblotting and immunofluorescence

HASM cells were serum starved for 48 hours followed by *Af* pretreatment for the indicated times. Lysates were prepared from cells, lungs, or BAL fluid using radioimmunoprecipitation (RIPA) lysis buffer supplemented with protease inhibitor and phosphatase inhibitor cocktails (Roche) and sonication. Primary antibody staining was

detected using near-infrared conjugated secondary antibodies and quantified with the LiCor Odyssey Imaging System and ImageStudio software (LiCor Biosciences). For immunofluorescent staining, cells were fixed in 3.7% paraformaldehyde and permeabilized with PBS containing 0.2% vol/vol Triton X-100. Cells were then blocked in 2% (wt/vol) BSA in PBS. Cells were incubated with mouse anti-vinculin antibody (1:100, Sigma) or rabbit anti-α9 integrin (Santa Cruz, 1:75) overnight at 4°C in blocking buffer. Cells were then incubated with AlexaFluor488-conjugated goat anti-mouse or goat anti-rabbit (1:200) secondary antibody followed by staining with Texas Red-conjugated phalloidin (Molecular Probes). Cells were mounted on coverglass with ProLong® Gold antifade reagent with DAPI. Images were obtained using the 63x oil immersion (NA 1.4, zoom 2) objective of a Leica SP5 confocal microscope and analyzed using Imaris software (BitPlane).

Mouse strains and asthma model

Eight to ten week-old female BALB/c mice (Jackson Laboratory) were sensitized intraperitoneally with *Af* crude extract (Hollister-Stier) [20 μg; 1.45×10^{-4} endotoxin units (EU)/μg, as determined by the ToxinSensor$_{TM}$ Chromogenic LAL Endotoxin Assay Kit (GenScript)] mixed with 20 mg Alum (Imject Alum, Pierce) on days 0 and 14. Mice were challenged intranasally with PBS ("naïve") or *Af* extract (25 μg, "acute") on days 25, 26 and 27. Mice were killed 24 hours after the last challenge. In some experiments, mice were treated intranasally with *Af* extract (25 μg) for 4 hours or overnight in the absence of sensitization. Another group of mice were treated intranasally with *Af* extract (50 μg) on days 0, 7 and 14 and then challenged with *Af* extract (20 μg) twice per week for 4 weeks followed by sacrifice 24 hours after last challenge ("chronic"). All studies were performed in accordance with institutional guidelines provided by the NIAID Animal Use and Care Committee under an approved study (ASP LAD3e).

Measurement of lung function in live anesthetized mice

Lung resistance (R_L), was recorded using the FlexiVent system (SCIREQ Scientific Respiratory Equipment, Inc.), as described previously[44].

Analysis of lung inflammation

Mouse lungs were perfused with 20 ml ice-cold PBS injected into left ventricle followed by excision and fixation in 10% neutral buffered formalin. Sections (5 μm) were prepared from paraffin-embedded lungs and stained with hematoxylin/eosin (H&E) and periodic acid Schiff (PAS). Images were obtained using a Leica DMI4000 light microscope equipped with Retiga2000R camera (QImaging, Canada) and analyzed by QCapture™ software. For analysis of BALF, mouse lungs were perfused with 1.5 ml ice cold HBSS, and lavage fluid was collected and centrifuged at 1500 rpm at 4°C for 10 min. Red blood cells in the pellet were lysed by ACK lysis buffer. Total cell number was determined by hemocytometry, and differentials were determined by light microscopic examination of a Diff-Quick (Siemens)-stained cytospin (700 cells in a minimum of 15 fields at 40x magnification).

Alp 1 localization

For immunostaining, mice were perfused through the left ventricle with PBS followed by lung excision and fixation in 10% neutral buffered formalin. Sections (5 μm) were prepared from paraffin-embedded lungs. Alp 1/*Asp f13* was detected by anti-Alp 1 antisera raised against a C-terminal peptide generated in rabbits (Yenzyme Antibodies LLC). Sections were counterstained with hematoxylin. Images were obtained using a Leica DMI4000 light microscope equipped with Retiga2000R camera (QImaging, Canada) and analyzed using QCapture™ software.

Human ASM experiments

HASM cells were extracted from lungs of de-identified healthy donors post-mortem obtained from the National Disease Research Interchange (NDRI) (Philadelphia, PA, USA). The isolation of ASM was performed in accordance with protocols approved by the Committee on Studies Involving Human Beings at the University of Pennsylvania_ENREF_33_ENREF_16. Cells were grown in Ham's F-12 media supplemented with 10% FBS and antibiotics. Cells were seeded in 96-well plates at 10,000 cells/well. Confluent monolayers were serum-starved for 48 hours followed by treatment with *Af* or vehicle (volumetric equivalent glycerol) for the indicated times. In some experiments *Af* extract was pre-incubated with PMSF (0.25 mM) or E-64 (10 μM) for 1 hour at room temperature or boiled for 30 minutes prior to cell stimulation. Plates were coated with different ECM proteins as follows: Collagens (I, III, IV) were prepared in 0.1 M acetic acid. Fibronectin was prepared in PBS. ECM proteins, PBS or 0.1 M acetic acid were incubated in wells overnight at 4°C. Wells were then incubated with 0.2% BSA in PBS for 30 minutes, washed with PBS, and air-dried prior to cell seeding.

Video microscopy

Cells were seeded on chambered coverglass slides (Lab-Tek, Nunc) and serum-starved for 48 hours. Differential interference contrast images were recorded every three minutes using a Leica AF6000LX confocal microscope with the 20X dry objective. Ten fields per well were visualized for each condition six minutes before and 28 hours after addition of vehicle or *Af* (10 μg ml^{-1}). Images were analyzed and movies recorded by Imaris software (BitPlane).

ECM proteolytic activity assay

Collagen I (20 μg) was prepared in buffer (50 mM Tris-HCl, 100 mM NaCl, 1.5 mM $CaCl_2$) and incubated with *Af* (20 μg) for 10 or 30 min or with collagenase D for 30 min at 37°C. Purified collagens I, III, IV, or fibronectin (20 μg) were incubated with vehicle or *Af* extract for 30 minutes at 37°C. Samples were boiled with sample buffer at 95°C, electrophoresed on 10% Tris-Glycine gels, and visualized by Coomassie Blue staining. HASM cells or mouse PCLS were incubated with *Af* extract for the indicated times. Acid-pepsin soluble collagen content was measured by Sircol assay (Biocolor).

Matrix metalloproteinase array

Serum-starved HASM cells were treated with vehicle or *Af* (2 μg ml^{-1}) for 24 hours. Relative amounts of MMPs and TIMPs in cell supernatants were determined using a Human MMP Antibody Array (Abcam,) according to the manufacturer's instructions. Blots were developed using biotinylated primary antibodies and streptavidin and quantified using Image Studio software.

Intracellular calcium measurements

HASM cells were seeded at low density (30–50% confluence) onto polystyrene vessel tissue culture-treated glass slides (BD Falcon) in Ham's F-12 medium supplemented with L-glutamine and 10% FBS for 24 hours at 37°C in 5% CO_2. Cells were starved in serum-free medium followed by treatment with vehicle or *Af* extract diluted in serum-medium for 24 hours at 37°C. F-12 media was replaced with 1:3 Fluo-8 (100 μL per chamber; Abcam Fluo-8 No Wash Calcium Assay Kit) in Ham's F-12 media. Cells were incubated in Fluo8 solution for 30 minutes then at room temperature in the dark for 30 minutes. Optical imaging (Nikon Eclipse TE2000-U Inverted Research Microscope) was performed immediately after the final incubation. Bradykinin (100 nM), histamine (10 μM), ionomycin (2 μM) or thapsigargin (100 nM) was added manually to the imaged chamber after 10 frames had been recorded, and images were recorded every second for 120 seconds. Mean, maximum, and minimum grayscale measurements were obtained for a cytoplasmic ROI for each responding cell in each frame using FIJI[18]. Mean grayscale measurements were adjusted for background and divided by the first frame. Results were plotted as mean normalized relative fluorescence units (fold-basal) ± s.e.m. *v*. time in seconds. In Fig. 3i, intracellular Ca^{2+} was measured in response to thrombin in cells plated in 96 well plates by fluorimetry as previously described[6].

Ins_{P1} measurements

HASM cells were seeded in 96-well plates and starved in serum-free media for 48 hours followed by 24 hours pre-treatment with vehicle or *Af* (2 μg ml^{-1}). Cells were then stimulated with increasing concentrations of bradykinin for two minutes. Ins_{P1} concentrations were measured by ELISA as described by the manufacturer (IP-One ELISA, Cisbio Bioassays).

$PI(4,5)P_2$ ELISA assay

HASM cells were seeded in 6-cm dishes and starved in serum-free media for 48 hours followed by pre-treatment with vehicle or *Af* (2 μg ml^{-1}) for indicated times. Extraction of $PI(4,5)P_2$–rich fractions and competitive ELISA assay were performed according to the manufacturer's instructions (Echelon Biosciences, kit# K-4500).

RhoA-GTP activation assay

HASM cells grown in 10-cm dishes were pre-treated with *Af* (2 μg ml^{-1}) for 24 hours and then stimulated with bradykinin (1 μM) for the indicated times. Cells were scraped into ice-cold MLB lysis buffer (Millipore) supplemented with NaF, Na_3VO_4, protease and phosphatase inhibitor cocktails (Roche). Lysates were clarified by centrifugation at 14,000 x

g for 5 min. Supernatants were incubated with GST-rhotekin Rho-binding domain according to the manufacturer's instructions (Millipore). Pull downs and total cell lysates were electrophoresed on 10% Tris-Glycine gels and immunoblotted with mouse anti-RhoA antibody. In a separate series of experiments, quantities of active RhoA and total RhoA were determined in cells treated as above using the appropriate G-LISA assay (Cytoskeleton). RhoA-GTP values were normalized to total RhoA for each sample.

ROCK and MLC activation assay

Cells were seeded onto CellStar tissue culture plates and grown to confluence in Ham's F-12 media supplemented with L-glutamine and 10% FBS at 37°C in 5% CO_2. Cells were starved in serum-free media for 72 hours at 37°C in 5% CO_2, then treated with vehicle, *Af* extract, or purified Alp 1 diluted in serum-free medium for 24 hours. Lysates were prepared in RIPA buffer and immunoblotted using the following primary antibodies: anti-pMYPT1 (T696) (Millipore), anti-pMLC2 (S18T19) (Cell Signaling Technologies) and anti-tubulin (Cell Signaling Technologies The following secondary antibodies were used: donkey anti-mouse (Jackson ImmunoResearch Laboratories, peroxidase-conjugated anti-mouse IgG or donkey anti-rabbit (Cell Signaling Technologies). Immunoblots were visualized using standard chemiluminescence protocols.

Flow cytometry

Serum-starved HASM cells were treated with *Af* (5 μg ml^{-1}) for 24 hours and then detached from the plate using a non-enzymatic solution (Cellstripper, Corning). For surface staining of F2R, cells were incubated with PE-conjugated mouse anti-F2R (1:15, R&D Systems) or the PE-conjugated isotype control (IgG2b 1:15) for 20 minute in FACS buffer at 4°C. Cells were then fixed in PBS containing 1% paraformaldehyde. For intracellular staining, cells were fixed and permeabilized in PBS containing 0.1% saponin and 0.05% BSA prior to staining. Fluorescence data were collected using an LSRII flow cytometer (BD Biosciences) and analyzed with Flowjo software (Tree Star, Inc., Ashland, OR).

Precision-cut lung slice airway contraction

Isolation and contraction of mouse PCLS were performed exactly as previously described with minor modifications[6]. After overnight incubation in serum-free medium, slices were treated with *Af* or vehicle for 24 hours. The next day, slices were washed with serum-free medium and used for the contraction assay. Images were obtained using a Leica DMI4000 light microscope equipped with Retiga2000R camera (QImaging, Canada) and analyzed using Image-pro Plus software (Media Cybernetics).

Immunohistochemistry

De-identified human lung specimens and clinical parameters were obtained from the Respiratory Health Network Tissue Bank of the Fonds de recherché québécois en santé, IUCPQ site (www.tissuebank.ca). The IUCPQ Ethics Committee approved the collection of tissue samples by the tissue bank and their use for these studies. All subjects gave informed consent for the tissue sampling and future use of samples for research purposes. Subjects with asthma were classified as having mild to moderate asthma based on criteria established

by the Global Initiative for Asthma (GINA). Human and mouse lung sections were deparaffinized and incubated with anti-Alp 1 rabbit antisera (1:1500) followed by DAB staining and hematoxylin counterstaining. In Image-pro Plus software, the Alp 1 positive pixels within ASM bundles were chosen using the “Segmentation” tool, and their area was measured by “Count and Measure Objects” tool and then normalized to the total ASM bundle area.

Protease activity assay

Protease activity was assessed using the Fluoro Protease Assay kit (G-Biosciences) according to the manufacturer’s instructions with minor modifications. Briefly, samples were diluted into 0.1 M Tris-HCl, pH 8.0 and added to wells of a 96-well black clear bottom Costar plate. FITC-conjugated casein assay substrate (100 μl [1 μg] diluted in 0.1 M Tris-HCl, pH 8.0) was added and incubated at room temperature for 30 minutes. Fluorescence intensity was determined using a Tecan Infinite M200 fluorescent reader at excitation/emission of 488/530 nm. Buffer without protease was used as a blank for background subtraction.

Purification of Alp 1 from *Aspergillus fumigatus* extracts

Af crude extract (50 ml, Hollister-Stier) was diluted into 25 mM acetic acid (200 ml) and applied to a HiPrep CM FF 16/10 column (GE Healthcare Bioscience) pre-equilibrated with 25 mM NaOAC-HAc, pH 4.8, with a peristaltic pump at 4°C. The column was then attached to an AKTA chromatographic system. After initial washing with equilibration buffer, bound proteins were eluted with a NaCl gradient (0-0.5 M NaCl) and fractions were collected and kept on ice. Aliquots of each fraction (1 μl) were analysed for protease activity as above. Proteolytically active fractions were combined and diluted with equilibration buffer then applied to two coupled HiTrap CM FF columns (GE Healthcare Bioscience) at 4°C. The coupled HiTrap CM FF columns were then attached to the AKTA chromatographic system and eluted with 0-0.5 M NaCl. Protease activity of each fraction was reanalyzed, and active fractions were combined and concentrated using Amicon Ultra-4 Centrifugal Filters (Millipore) by centrifugation in a tabletop centrifuge (2350 x *g*) for each run. The concentrated fraction (approximate 400 μl final volume) was applied to two column-coupled Superdex 75 10/300GL columns. The columns were pre-equilibrated with 25 mM NaOAc-HAc buffer, pH 4.8 and eluted with same buffer. The fractions were collected and re-analysed for protease activity. The final active fractions were combined and the purity determined by SDS-PAGE. Bands detected by Coomassie blue staining of SDS-PAGE gels were excised and subjected to mass spectrometric protein identification.

Mass spectrometry and protein identification

Identification of all SDS-PAGE separated proteins was performed on reduced and alkylated, trypsin digested samples prepared by standard mass spectrometry protocols. The supernatant and two washes (5% formic acid in 50% acetonitrile) of the gel digests were pooled and concentrated by speed vacuum centrifugation (Labconco) to dryness directly in 200 μl polypropylene auto-sampler vials (Sun Sri, Rockwood, TN). Recovered peptides were re-suspended in 5 μl of Solvent A (0.1% formic acid, 2% acetonitrile, and 97.9% water). Prior

to mass spectrometry analysis, the re-suspended peptides were chromatographed directly on column, without trap cleanup. The bound peptides were separated using AQ C18 reverse phase media (3 μm particle size and 200 μm pore; 500 nl per min generating 80–120 Bar pressure) packed in a pulled tip, nano-chromatography column (0.1 mm ID x 150 mm L) from Precision Capillary Columns. Chromatography was performed in-line with an LTQ-Velos Orbitrap mass spectrometer (ThermoFisher Scientific), and the mobile phase consisted of a linear gradient prepared from solvent A and solvent B (0.1% formic acid, 2% water, 97.9% acetonitrile) at room temperature. Nano LC-MS (LC-MS/MS) was performed with a ProXeon Easy-nLC II multi-dimensional liquid chromatograph and temperature controlled Ion Max Nanospray source (ThermoFisher Scientific) in-line with the LTQ-Velos Orbitrap mass spectrometer. Computer controlled data-dependent automated switching to MS/MS by Xcalibur 2.1 software was used for data acquisition and provided peptide sequence information. Data processing and databank searching were performed with PD 1.2 and Mascot software (Matrix Science). Data were searched against protein sequences deposited in the National Center for Biotechnology Information non-redundant protein database (NCBInr, 04/2011) and a reverse sequence decoy database. Proteins were identified using a 1% False Discovery Rate cutoff and 2 peptides per protein minimum.

Cell viability assay

HASM cells were seeded in 96-well plates and serum-starved for 48 hours. Cells were treated with vehicle, *Af* (5 μg ml^{-1}) or heat-inactivated *Af*. The metabolic activity of cells was measured using CellTiter-Glo® Luminescent Cell Viability Assay (Promega).

AnnexinV/PI staining

HASM cells were seeded in 4-well chamber slides (Lab-Tek, Nunc) and serum-starved for 48 hours. Cells were left untreated or treated with vehicle, *Af* (5 μg ml^{-1}) for 48 hours or with staurosporine (1 μM) for 6 hours. Cells were then stained with FITC-conjugated Annexin V-antibody and propidium iodide (PI) as described by the manufacturer (BD Biosciences). Images were obtained using a Leica DMI4000 Fluorescence microscope equipped with Retiga2000R camera (QImaging, Canada) and analyzed using Image-pro Plus software (Media Cybernetics).

Caspase 3/7 activity

HASM cells were seeded in 96-well plates, serum-starved for 48 hours and treated with vehicle, *Af* (5 μg ml^{-1}) or heat-inactivated *Af* or staurosporine (1 μM). Caspase3/7 activity was measured by luminescence assay as an indicator of apoptosis as described by the manufacturer (Caspase-Glo® 3/7 Assay, Promega).

EdU staining

HASM cells were seeded in 4-well chamber slides (Lab-Tek, Nunc). Cells were serum starved for 48 hours and left untreated or treated with vehicle, *Af* (5 μg ml^{-1}) or PDGF (50 ng ml^{-1}) for 48 hours. 5-ethynyl-2′-deoxyuridine (EdU) incorporation was measured using the Click-iT® EdU Imaging Kit (Molecular Probes) by microscopy on coverglass slides mounted with ProLong® Gold antifade reagent with DAPI.

Statistical analysis

GraphPad Prism software was used for data analysis. Statistical significance was determined using student's *t* test (for two groups) or one- or two-way ANOVA for multiple groups. Non-parametric Kruskal Wallis tests were used to compare the human lung samples. *P* values less than 0.05 were considered significant.

Supplementary Material

Refer to Web version on PubMed Central for supplementary material.

Acknowledgments

This research was supported in part by the Intramural Research Program of the NIH, NIAID, and by NIH grants P01-HL114471 and P30-ES013508 (to R.A.P.). We thank Lisa R. Olano, Ph.D. (Protein Chemistry, Research Technologies Branch, NIAID/NIH) for assistance with mass spectrometry; Sabrina Biardel and Dr. Jamila Chakir (IUPSQ) for assistance in obtaining human samples. We thank Sundar Ganesan, Ph.D. (Biological Imaging, Research Technologies Branch, NIAID/NIH) for assistance with confocal microscopy. We express our gratitude to Dr. Axel A. Brakhage (Leibniz Institute for Natural Product Research and Infection Biology, Germany) for providing reagents. We thank Dr. Helene Rosenberg (NIAID/NIH) for critical review of the manuscript and Drs. Juraj Kabat and Olena Kamenyeva for assistance with confocal imaging.

References

1. West AR, et al. Airway contractility and remodeling: links to asthma symptoms. Pulmonary pharmacology & therapeutics. 2013; 26:3–12. [PubMed: 22989721]
2. Hirota N, Martin JG. Mechanisms of airway remodeling. Chest. 2013; 144:1026–1032. [PubMed: 24008953]
3. Prakash YS. Airway smooth muscle in airway reactivity and remodeling: what have we learned? American journal of physiology. Lung cellular and molecular physiology. 2013; 305:L912–L933. [PubMed: 24142517]
4. Reddel CJ, Weiss AS, Burgess JK. Elastin in asthma. Pulmonary pharmacology & therapeutics. 2012; 25:144–153. [PubMed: 22366197]
5. Albacker LA, et al. Invariant natural killer T cells recognize a fungal glycosphingolipid that can induce airway hyperreactivity. Nature medicine. 2013; 19:1297–1304.
6. Balenga NA, Jester W, Jiang M, Panettieri RA Jr, Druey KM. Loss of regulator of G protein signaling 5 promotes airway hyperresponsiveness in the absence of allergic inflammation. The Journal of allergy and clinical immunology. 2014
7. Lambrecht BN, Hammad H. The immunology of asthma. Nature immunology. 2014; 16:45–56. [PubMed: 25521684]
8. Millien VO, et al. Cleavage of fibrinogen by proteinases elicits allergic responses through Toll-like receptor 4. Science. 2013; 341:792–796. [PubMed: 23950537]
9. Chiu LL, Perng DW, Yu CH, Su SN, Chow LP. Mold allergen, pen C 13, induces IL-8 expression in human airway epithelial cells by activating protease-activated receptor 1 and 2. Journal of immunology. 2007; 178:5237–5244.
10. Chen JC, et al. The protease allergen Pen c 13 induces allergic airway inflammation and changes in epithelial barrier integrity and function in a murine model. The Journal of biological chemistry. 2011; 286:26667–26679. [PubMed: 21613216]
11. Leino MS, et al. Barrier disrupting effects of alternaria alternata extract on bronchial epithelium from asthmatic donors. PloS one. 2013; 8:e71278. [PubMed: 24009658]
12. Kheradmand F, et al. A protease-activated pathway underlying Th cell type 2 activation and allergic lung disease. Journal of immunology. 2002; 169:5904–5911.

13. Moser M, Menz G, Blaser K, Crameri R. Recombinant expression and antigenic properties of a 32-kilodalton extracellular alkaline protease, representing a possible virulence factor from Aspergillus fumigatus. Infection and immunity. 1994; 62:936–942. [PubMed: 8112866]
14. Latge JP. The pathobiology of Aspergillus fumigatus. Trends in microbiology. 2001; 9:382–389. [PubMed: 11514221]
15. Kauffman HF, Tomee JF, van de Riet MA, Timmerman AJ, Borger P. Protease-dependent activation of epithelial cells by fungal allergens leads to morphologic changes and cytokine production. The Journal of allergy and clinical immunology. 2000; 105:1185–1193. [PubMed: 10856154]
16. Dekkers BG, Schaafsma D, Nelemans SA, Zaagsma J, Meurs H. Extracellular matrix proteins differentially regulate airway smooth muscle phenotype and function. American journal of physiology. Lung cellular and molecular physiology. 2007; 292:L1405–L1413. [PubMed: 17293376]
17. Kremer SG, Breuer WV, Skorecki KL. Vasoconstrictor hormones depolarize renal glomerular mesangial cells by activating chloride channels. Journal of cellular physiology. 1989; 138:97–105. [PubMed: 2536039]
18. Pelaia G, et al. Molecular mechanisms underlying airway smooth muscle contraction and proliferation: implications for asthma. Respiratory medicine. 2008; 102:1173–1181. [PubMed: 18579364]
19. Penn RB, Benovic JL. Regulation of heterotrimeric G protein signaling in airway smooth muscle. Proceedings of the American Thoracic Society. 2008; 5:47–57. [PubMed: 18094084]
20. Zhang W, Gunst SJ. Interactions of airway smooth muscle cells with their tissue matrix: implications for contraction. Proceedings of the American Thoracic Society. 2008; 5:32–39. [PubMed: 18094082]
21. Gunst SJ, Zhang W. Actin cytoskeletal dynamics in smooth muscle: a new paradigm for the regulation of smooth muscle contraction. American journal of physiology. Cell physiology. 2008; 295:C576–C587. [PubMed: 18596210]
22. Chen C, et al. Integrin alpha9beta1 in airway smooth muscle suppresses exaggerated airway narrowing. The Journal of clinical investigation. 2012; 122:2916–2927. [PubMed: 22772469]
23. Iadarola P, et al. Lung injury and degradation of extracellular matrix components by Aspergillus fumigatus serine proteinase. Experimental lung research. 1998; 24:233–251. [PubMed: 9635248]
24. Elshaw SR, et al. Matrix metalloproteinase expression and activity in human airway smooth muscle cells. British journal of pharmacology. 2004; 142:1318–1324. [PubMed: 15265805]
25. Xie S, et al. Induction and regulation of matrix metalloproteinase-12 in human airway smooth muscle cells. Respiratory research. 2005; 6:148. [PubMed: 16359550]
26. Altraja A, et al. Expression of laminins in the airways in various types of asthmatic patients: a morphometric study. American journal of respiratory cell and molecular biology. 1996; 15:482–488. [PubMed: 8879182]
27. Hirst SJ, Twort CH, Lee TH. Differential effects of extracellular matrix proteins on human airway smooth muscle cell proliferation and phenotype. American journal of respiratory cell and molecular biology. 2000; 23:335–344. [PubMed: 10970824]
28. Roche WR, Beasley R, Williams JH, Holgate ST. Subepithelial fibrosis in the bronchi of asthmatics. Lancet. 1989; 1:520–524. [PubMed: 2466184]
29. Sanderson MJ, Delmotte P, Bai Y, Perez-Zogbhi JF. Regulation of airway smooth muscle cell contractility by Ca2+ signaling and sensitivity. Proceedings of the American Thoracic Society. 2008; 5:23–31. [PubMed: 18094081]
30. Perez JF, Sanderson MJ. The frequency of calcium oscillations induced by 5-HT, ACH, and KCl determine the contraction of smooth muscle cells of intrapulmonary bronchioles. The Journal of general physiology. 2005; 125:535–553. [PubMed: 15928401]
31. Sandhaus RA, Turino G. Neutrophil elastase-mediated lung disease. Copd. 2013; (10 Suppl 1):60–63. [PubMed: 23527919]
32. Khan MA, Kianpour S, Stampfli MR, Janssen LJ. Kinetics of in vitro bronchoconstriction in an elastolytic mouse model of emphysema. The European respiratory journal. 2007; 30:691–700. [PubMed: 17537774]

33. Qian SY, Mitzner W. In vivo and in vitro lung reactivity in elastase-induced emphysema in hamsters. The American review of respiratory disease. 1989; 140:1549–1555. [PubMed: 2690702]
34. Kudo M, et al. Mfge8 suppresses airway hyperresponsiveness in asthma by regulating smooth muscle contraction. Proceedings of the National Academy of Sciences of the United States of America. 2013; 110:660–665. [PubMed: 23269839]
35. Dekkers BG, et al. Focal adhesion kinase regulates collagen I-induced airway smooth muscle phenotype switching. The Journal of pharmacology and experimental therapeutics. 2013; 346:86–95. [PubMed: 23591997]
36. Kurup VP, et al. Alkaline serine proteinase from Aspergillus fumigatus has synergistic effects on Asp-f-2-induced immune response in mice. International archives of allergy and immunology. 2002; 129:129–137. [PubMed: 12403930]
37. Oguma T, et al. Induction of mucin and MUC5AC expression by the protease activity of Aspergillus fumigatus in airway epithelial cells. Journal of immunology. 2011; 187:999–1005.
38. Borger P, et al. Proteases from Aspergillus fumigatus induce interleukin (IL)-6 and IL-8 production in airway epithelial cell lines by transcriptional mechanisms. The Journal of infectious diseases. 1999; 180:1267–1274. [PubMed: 10479157]
39. Kogan TV, Jadoun J, Mittelman L, Hirschberg K, Osherov N. Involvement of secreted Aspergillus fumigatus proteases in disruption of the actin fiber cytoskeleton and loss of focal adhesion sites in infected A549 lung pneumocytes. The Journal of infectious diseases. 2004; 189:1965–1973. [PubMed: 15143461]
40. Porter PC, et al. Airway surface mycosis in chronic TH2-associated airway disease. The Journal of allergy and clinical immunology. 2014; 134:325–331. [PubMed: 24928648]
41. Kauffman HF, Tomee JF, van der Werf TS, de Monchy JG, Koeter GK. Review of fungus-induced asthmatic reactions. American journal of respiratory and critical care medicine. 1995; 151:2109–2115. discussion 2116. [PubMed: 7767565]
42. Miglino N, Roth M, Tamm M, Borger P. House dust mite extract downregulates C/EBPalpha in asthmatic bronchial smooth muscle cells. The European respiratory journal. 2011; 38:50–58. [PubMed: 21109558]
43. Wenzel SE. Complex phenotypes in asthma: current definitions. Pulmonary pharmacology & therapeutics. 2013; 26:710–715. [PubMed: 23880027]
44. Haczku A, et al. Hyperpolarized 3He MRI in asthma measurements of regional ventilation following allergic sensitization and challenge in mice--preliminary results. Academic radiology. 2005; 12:1362–1370. [PubMed: 16253848]

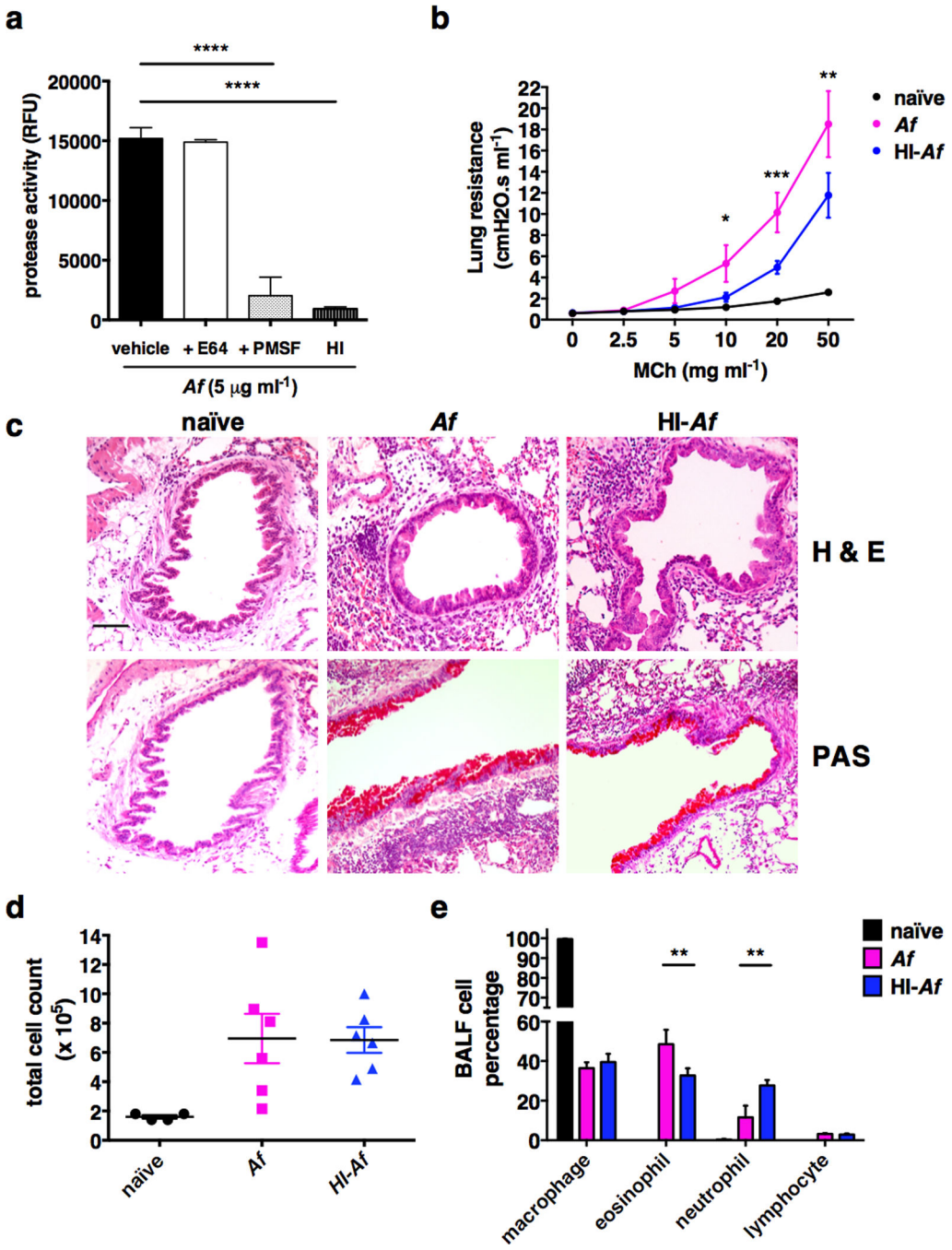

Figure 1. *Af* protease activity promotes AHR

(**a**) Protease activity in crude *Af* extracts incubated with vehicle alone, PMSF (serine protease inhibitor, 250 μM), E64 (cysteine protease inhibitor, 10 μM) or heat-inactivated (HI)-*Af*] was determined as described in Methods. Bar graph shows mean ± s.e.m. of three independent experiments (****$P < 0.0001$, one-way ANOVA). (**b**) Lung resistance (RL) in response to aerosolized methacholine (MCh) was measured in naïve, *Af* or HI-*Af* sensitized and challenged BALB/c WT mice 24 hours after the final challenge. Data in (b–e) are mean ± s.e.m of 4-6 mice per group measured in a single experiment (*$P = 0.04$, **$P = 0.001$,

***P = 0.0006, two-way ANOVA, comparing *Afv*. HI *Af*). (**c**) Peribronchial infiltration and goblet cell metaplasia of paraffin-embedded mouse lungs were evaluated by using hematoxylin/eosin and Periodic acid-Schiff staining, respectively (Scale bar 100 μm, original magnification 10x). (**d**) Total cell counts and (**e)** differentials were assessed in BALF cytospin preparations. (**P < 0.01 two-way ANOVA).

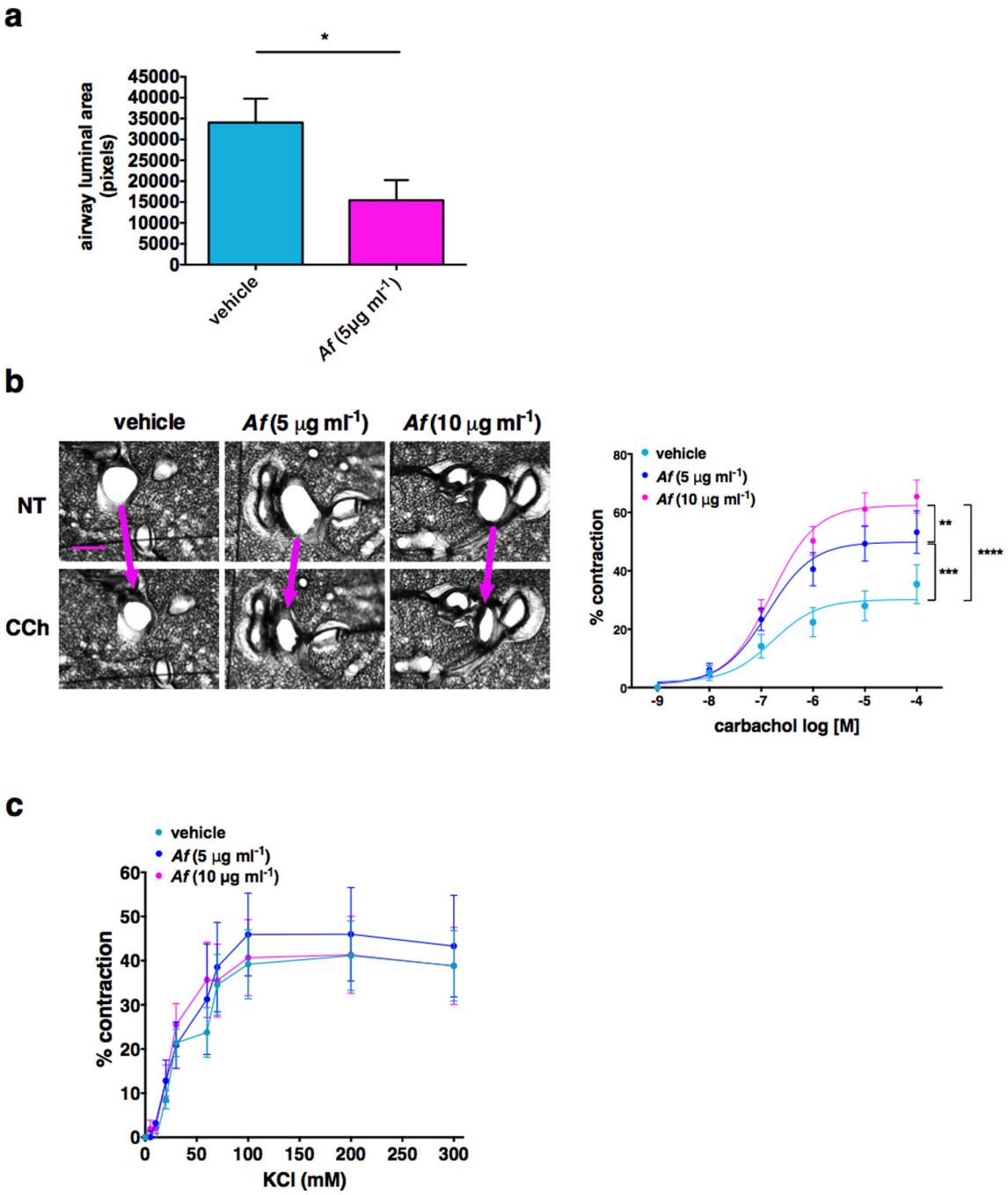

Figure 2. *Af* induces bronchoconstriction in PCLS

Mouse lung slices were pre-treated with vehicle or *Af* (5 or 10 μg/ml) for 24 hours. (**a**) Bright field images of airways in PCLS treated with vehicle or *Af* (5 μg ml^{-1}) were obtained and used to calculate baseline airway luminal areas as per the Methods. (mean ± s.e.m of 26–45 airways evaluated in 2-3 experiments; **P* = 0.03, *t* test). (**b**) Left panel: Bright field images were obtained before (NT) and four minutes after carbachol (CCh, 100 μM) stimulation. Scale bar, 300 μm; original magnification, 5x. Arrows denote contracting airways. Right panel: Slices were stimulated with increasing concentrations of CCh, and

percent contraction was calculated based on the airway luminal area. Data are expressed as mean ± s.e.m. of three independent experiments (23–25 airways per group) fitted to a curve using the least-squares fit method. E_{max} was compared between groups by extra sum-of-square F test (***P* < 0.01, ****P* < 0.001, *****P* < 0.0001, two-way ANOVA). (**c**) PCLS were prepared as in (a) and stimulated with the indicated concentrations of KCl. Data are mean ± s.e.m. of two independent experiments (9–15 airways per group).

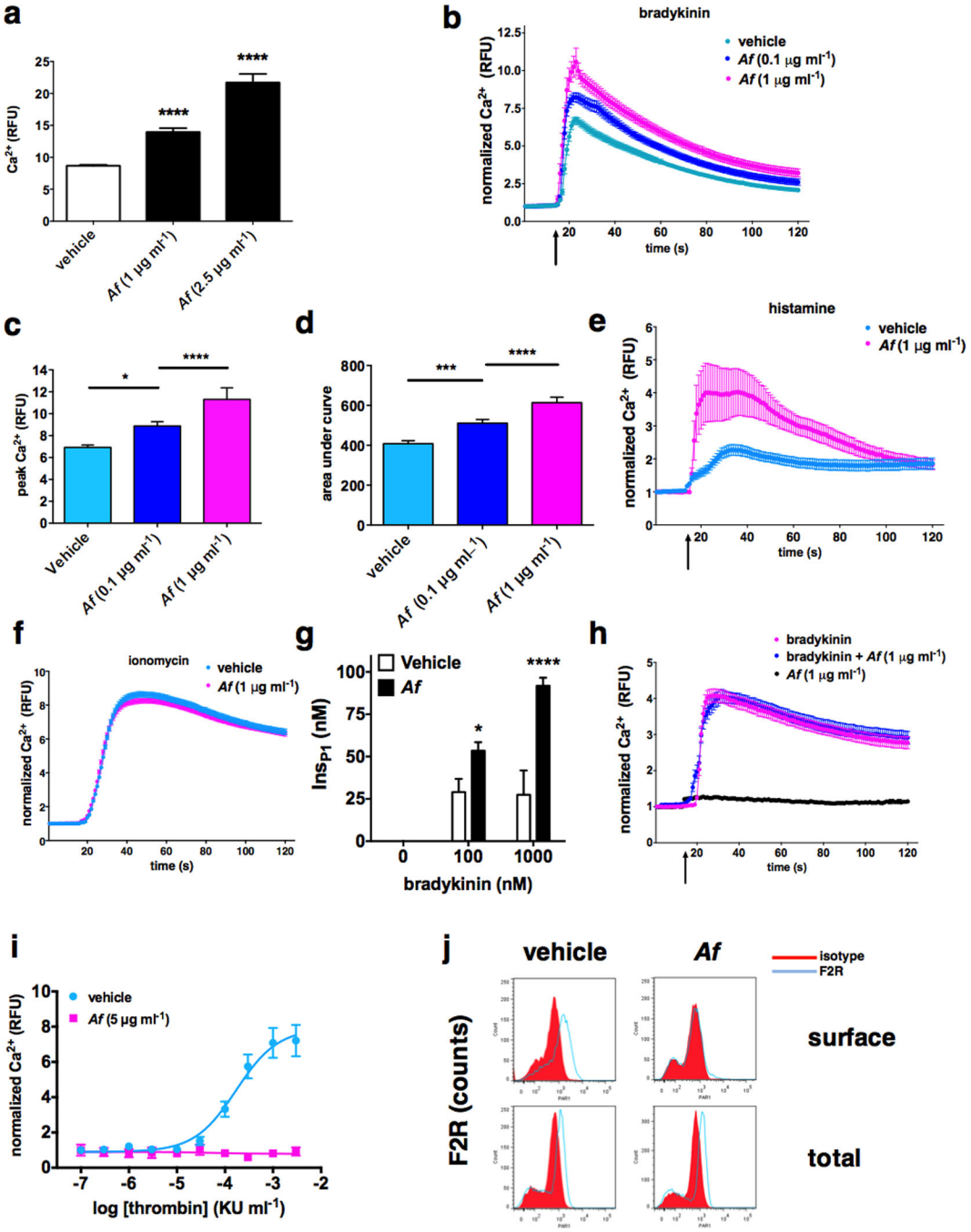

Figure 3. *Af* modulates Ca^{2+} mobilization in ASM cells

Serum-starved HASM cells were left untreated or pre-incubated with *Af* extract for 24 hours prior to measurement of cytosolic Ca^{2+} by fluorescence microscopy as outlined in the Methods. (**a**) Baseline Ca^{2+} levels after treatments are shown as mean ± s.e.m. of a minimum of 60 cells/condition measured in three independent experiments (*****P* < 0.0001, one-way ANOVA). (**b**-**f**) Agonist-induced Ca^{2+} mobilization. Line graphs in (b) (bradykinin, 100 nM), (e) (histamine, 10 μM), (f) (ionomycin, 2 μM), show normalized Ca^{2+} measurements over time (mean ± s.e.m. of 16–80 cells measured in 2-3 independent

experiments) at baseline and following addition of agonist (arrows). (**c**) Peak and area under curve (**d**) of Ca^{2+} spikes in (b) were calculated (**P* = 0.03, ****P* = 0.0005 *****P* < 0.0001, one-way ANOVA). (**g**) Serum-starved HASM cells were pretreated with vehicle or *Af* (2 μg ml^{-1}) for 24 hours. Accumulation of Ins_{P1} was measured after addition of the indicated concentrations of bradykinin. Data are mean ± s.e.m. of three independent experiments (**P* = 0.04, ****P* < 0.0001, two-way ANOVA). (**h**) HASM cells were stimulated acutely with *Af*, bradykinin (100 nM), or *Af* + bradykinin (100 nM) followed by measurement of Ca^{2+} by microscopy as in (b-f**)**. Graph represents mean ± s.e.m. of 7–60 cells per condition. (**i**) HASM cells were pretreated with vehicle or *Af* (5 μg ml^{-1}) for 24 hours followed by stimulation with thrombin and measurement of Ca^{2+} mobilization by fluorimetry. Normalized Ca^{2+} values are mean ± s.e.m. of a single experiment representative of two independent experiments. (**j**) Surface and total F2R receptor expression in vehicle or *Af*-treated HASM cells was measured by flow cytometry. Representative histograms from 2–3 independent experiments are shown.

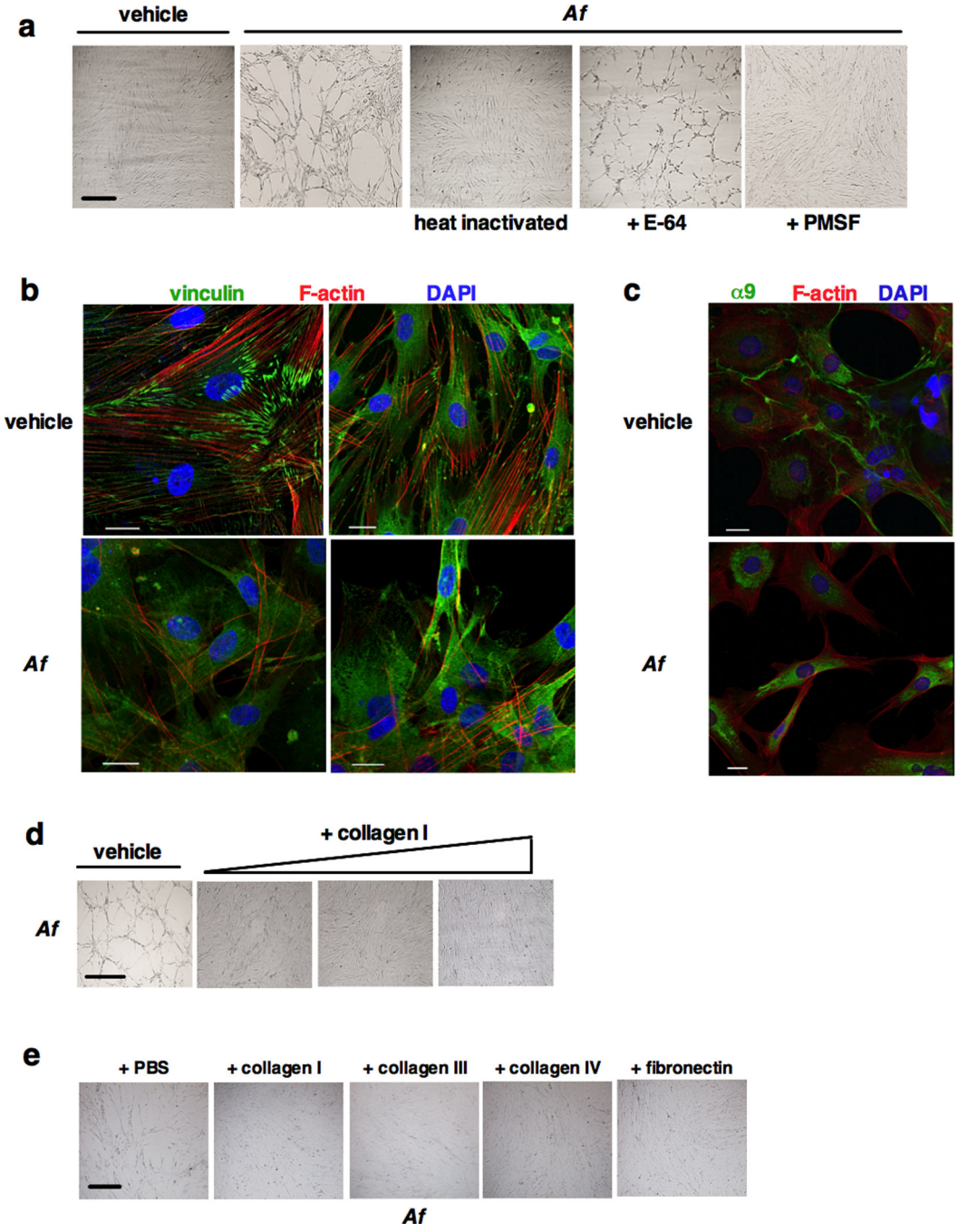

Figure 4. *Af* serine protease activity induces morphological changes in ASM cells

(**a**) Serum-starved HASM cells were treated with vehicle, unmodified *Af* (5 μg ml^{-1}), HI-*Af*, or *Af* incubated with PMSF (250 μM) or E-64 (10 μM) protease inhibitors. Scale bar, 200 μm; original magnification, 10x. **(b–c)** Serum-starved HASM cells (b) or mouse ASM cells (c) were treated with vehicle or *Af* (5 μg ml^{-1}) for 24 hours. Fixed cells were stained with phalloidin (red) and anti-vinculin antibody (green) (b) or α9-integrin antibody (c). Nuclei were counterstained with DAPI. Images in (b–c) are from a single experiment representative of 2-3 similar experiments. Scale bar, 20 μm; original magnification, 63x. (**d**) HASM cells

were cultured on plates coated with collagen I (0.2-1 mg ml^{-1}) followed by treatment with *Af* (5 μg ml^{-1}) for 48 hours. DIC images are from a single experiment representative of three similar experiments. Scale bar, 200 μm; original magnification, 10x. (**e**) HASM cells were seeded on plates coated with collagen I (1 mg ml^{-1}), collagen III (0.1 mg ml^{-1}), collagen IV (0.5 mg ml^{-1}) or fibronectin (0.1 mg ml^{-1}). After serum starvation, cells were treated with *Af* (5 μg ml^{-1}) and visualized by microscopy 48 hours post treatment. Scale bar, 200 μm; original magnification, 10x. Images are from a single experiment representative of 2–4 independent experiments.

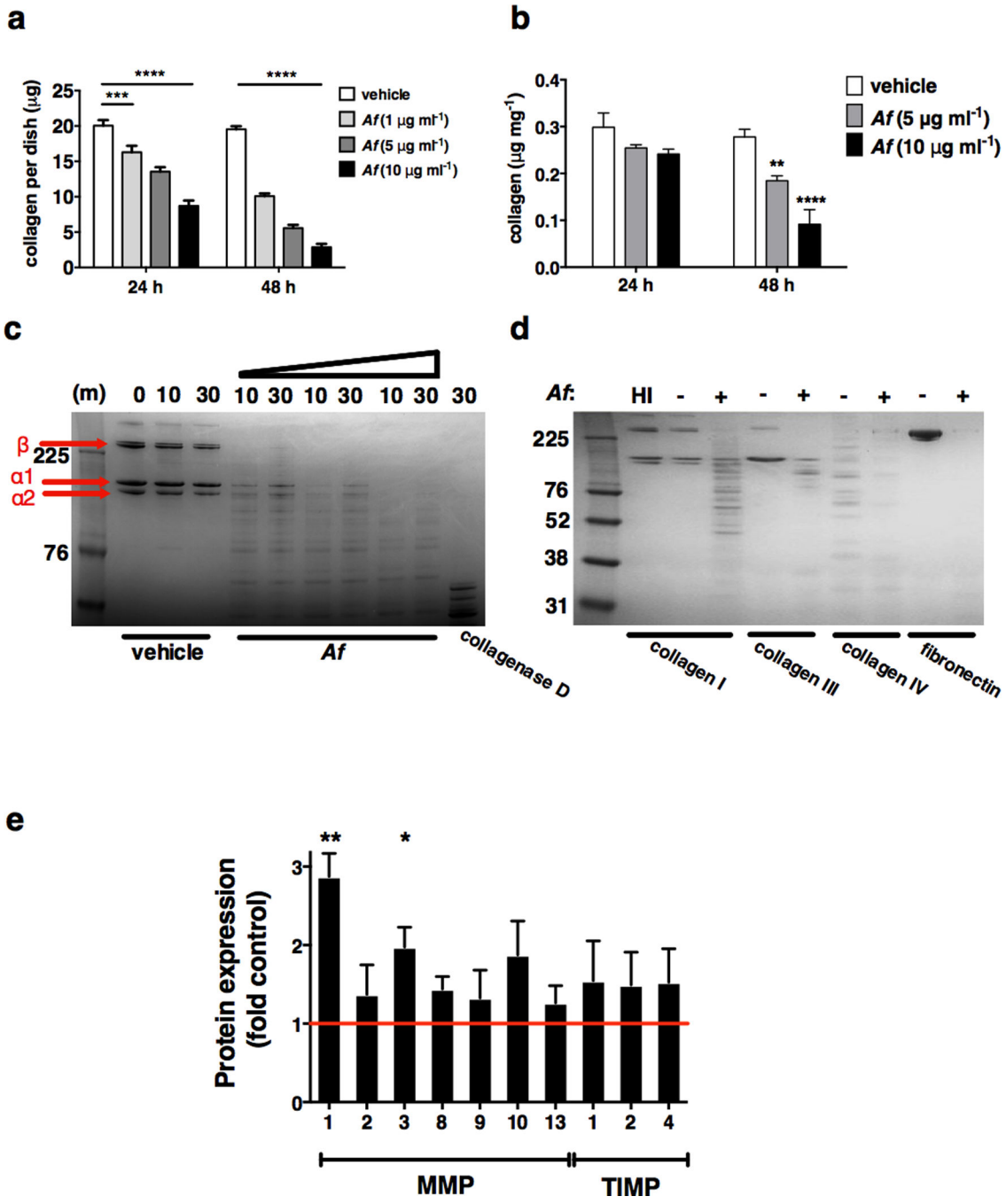

Figure 5. *Af* degrades the extracellular matrix

(**a**) Total collagen content in cultured HASM cells left untreated or incubated with *Af* for the indicated times. Graph shows mean ± s.e.m. from a single experiment representative of three independent experiments (***$P = 0.006$, ****$P < 0.0001$, two-way ANOVA). (**b**) Collagen content in PCLS left untreated or incubated with *Af* for the indicated times; data are mean ± s.e.m. of three independent experiments (**$P = 0.007$; ***$P < 0.0001$, two-way ANOVA). (**c**) Vehicle, *Af* (5, 10 or 20 µg) or collagenase D (50 µg) was incubated with collagen I (20 µg) for the indicated times at 37°C. Samples were resolved by SDS-PAGE and visualized by

Coomassie staining. α1, α2 and β subunits of collagen I are denoted by red arrows. **(d)** Vehicle, *Af* (20 μg ml^{-1}) or heat-inactivated *Af* (HI-*Af*, 20 μg ml^{-1}) were incubated with of collagens I, III, IV, or fibronectin (20 μg) for 30 min at 37°C. (**e**) Secretion of MMPs and TIMPs in cell supernatants was measured by antibody array. Bar graph depicts relative expression (mean ± s.e.m. of three independent experiments) in *Af*-treated HASM cells compared to control (***P* =0.003, **P* = 0.01, *t* test).

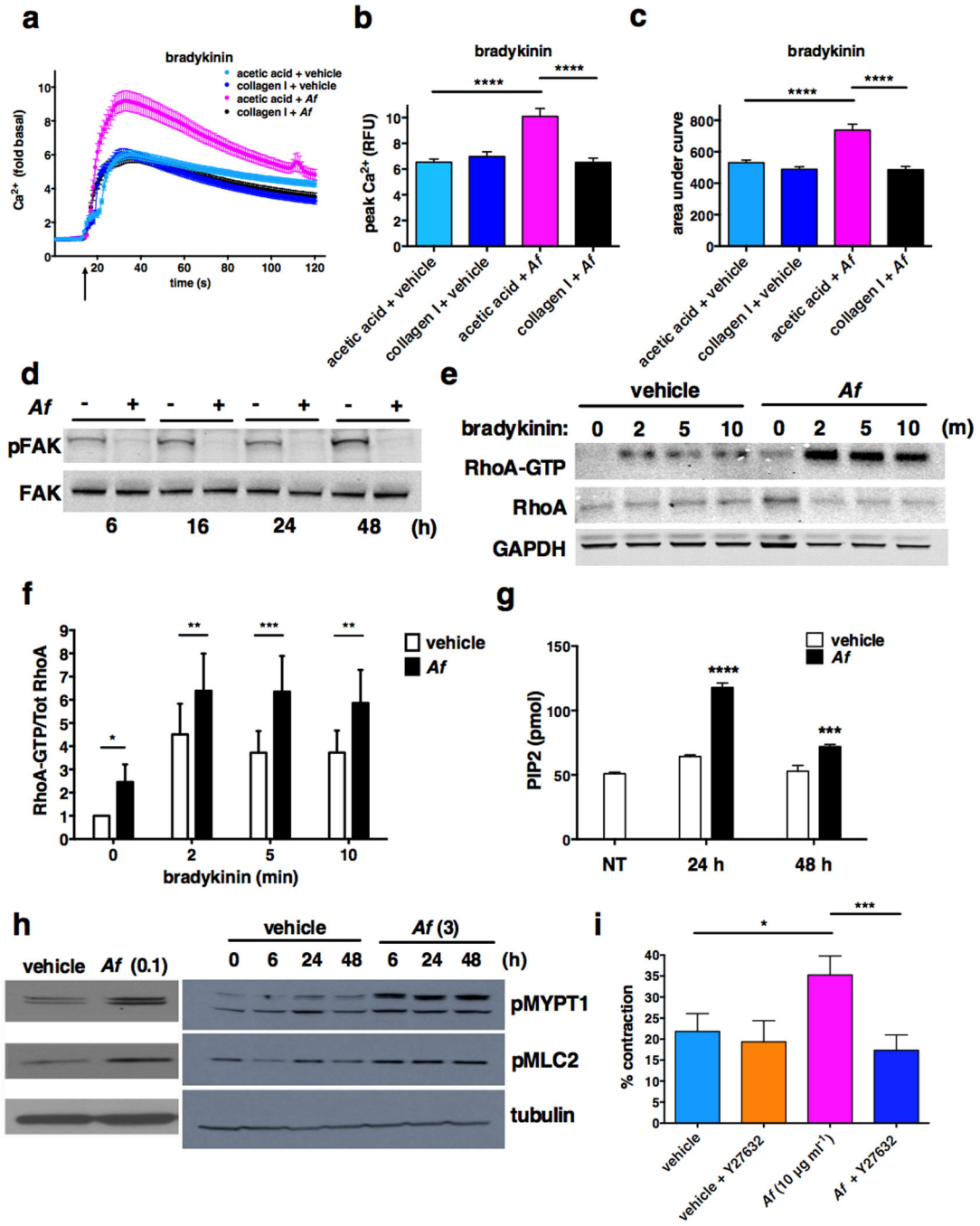

Figure 6. *Af* enhances Ca^{2+} sensitivity in ASM downstream of FAK and ROCK

(**a-c)** HASM cells were seeded on tissue culture plates pre-coated with vehicle (acetic acid) or collagen I (50 μg/ml). Serum-starved cells were treated with vehicle or *Af* (1 μg/ml) for 24 hours. Cytosolic calcium was measured in individual cells following bradykinin stimulation as in Figure 3. Data are mean ± s.e.m. of 80-100 cells from two individual donors measured in two independent experiments (***P* < 0.01, ****P* < 0.001, one-way ANOVA). (**d**) HASM cells were treated with vehicle or *Af* (2 μg ml^{-1}) for the indicated times followed by assessment of FAK phosphorylation and expression by immunoblotting. (**e-f**) HASM cells

were treated with vehicle or *Af* (2-3 μg ml^{-1}) followed by stimulation with bradykinin (1 μM) for the indicated times. GTP-bound and total RhoA were assessed by pull-down, immunoblotting, and ELISA. Bar graph data are mean ± s.e.m. of eight experiments (**P* = 0.04, ***P* < 0.008; ****P* = 0.0007, two-way ANOVA). (**g**) Serum-starved HASM cells were pretreated with vehicle or *Af* (2 μg ml^{-1}) for the times indicated. PIP2 concentrations in cell extracts were determined by ELISA. Data are mean ± s.e.m. of three independent experiments (****P* < 0.001, *****P* < 0.0001, one-way ANOVA). (**h**) HASM cells were pretreated with vehicle or *Af* (0.1-3 μg ml^{-1}) for the times indicated. MYPT1 and MLC2 phosphorylation was assessed in whole cell lysates by immunoblotting. Blots are from a single experiment representative of 3-6 independent experiments. (**i**) Mouse PCLS were pre-treated with vehicle or *Af* (10 μg/ml) for 24 hours. Slices were treated with vehicle or ROCK inhibitor (Y27632, 10 μM) one hour prior to stimulation with CCh (100 nM) and measurement of airway contraction. Data are mean ± s.e.m. of two independent experiments using 4 mice in each (16-20 airways/condition; **P* = 0.03, ***P* = 0.003, one-way ANOVA).

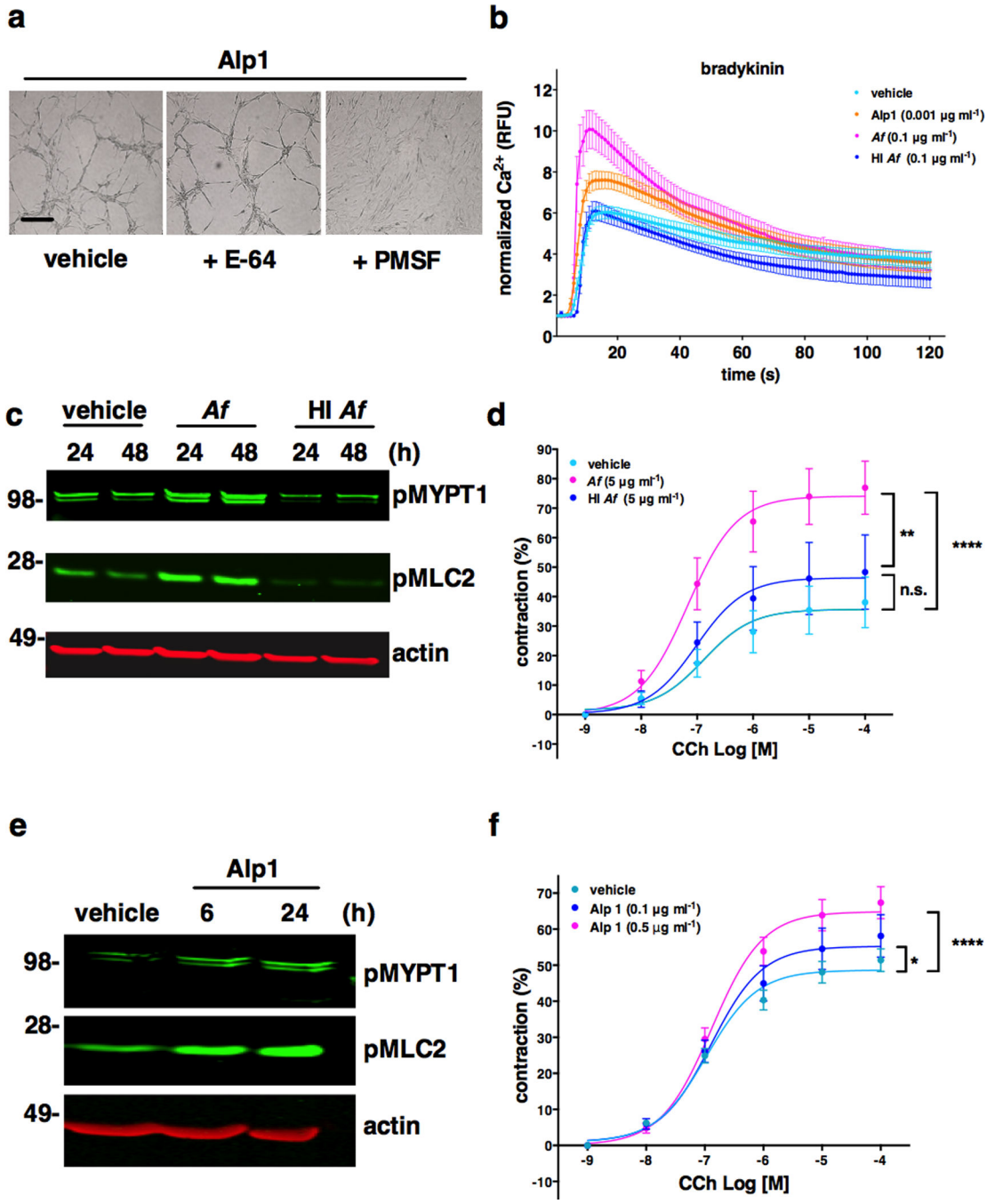

Figure 7. Alp 1 serine protease regulates Ca^{2+} sensitivity in ASM

(**a**) HASM cells were treated with purified Alp 1 (3 µg ml^{-1}) in the presence or absence of serine (PMSF, 250 µM) or cysteine (E-64, 10 µM) protease inhibitors for 48 hours. DIC images are from a single experiment representative of three similar experiments. (**b**) Serum-starved HASM cells were pre-incubated with vehicle, untreated *Af* extract, heat-inactivated *Af*, or purified Alp 1 at the concentrations indicated for 24 hours prior to measurement of cytosolic Ca^{2+} in individual cells following bradykinin (100 nM) stimulation as in Figure 3. Data are mean ± s.e.m. of 12-25 cells from two individual donors measured in two

independent experiments ($P < 0.0001$, two-way ANOVA, vehicle *vAf* or Alp 1). (**c**) HASM cells were treated with vehicle, *Af*, or HI *Af* (3 μg ml^{-1}) for the indicated times, and phosphorylation of MYPT1 and MLC2 was assessed by immunoblotting. Images are from a single experiment representative of three independent experiments. (**d**) PCLS were prepared from naïve mice and pre-treated with vehicle, *Af*, or HI Af (5 μg/ml) for 24 hours. Slices were stimulated with increasing concentrations of CCh and percent contraction calculated as in Figure 1. Data (mean ± s.e.m.) are from a single experiment using four mice representative of two similar experiments (7-11 airways per group) fitted to a curve using the least-squares fit method. E_{max} was compared between groups by extra sum-of-square F test; n.s,, not significant (**$P = 0.001$; ****$P < 0.0001$, two-way ANOVA). (**e**) HASM cells were treated with vehicle or Alp 1 (1 μg ml^{-1}) for the indicated times, and phosphorylation of MYPT1 and MLC2 was assessed by immunoblotting. Images are from a single experiment representative of three independent experiments. (**f**) PCLS were prepared from naïve mice and pre-treated with vehicle or purified Alp 1 (0.1 or 0.5 μg ml^{-1}) for 24 hours. Slices were stimulated with increasing concentrations of CCh and analyzed as in (d). Data (mean ± s.e.m.) are from three experiments using 2-4 mice in each (30-80 airways/ condition; *$P = 0.03$; ****$P < 0.0001$, two-way ANOVA).

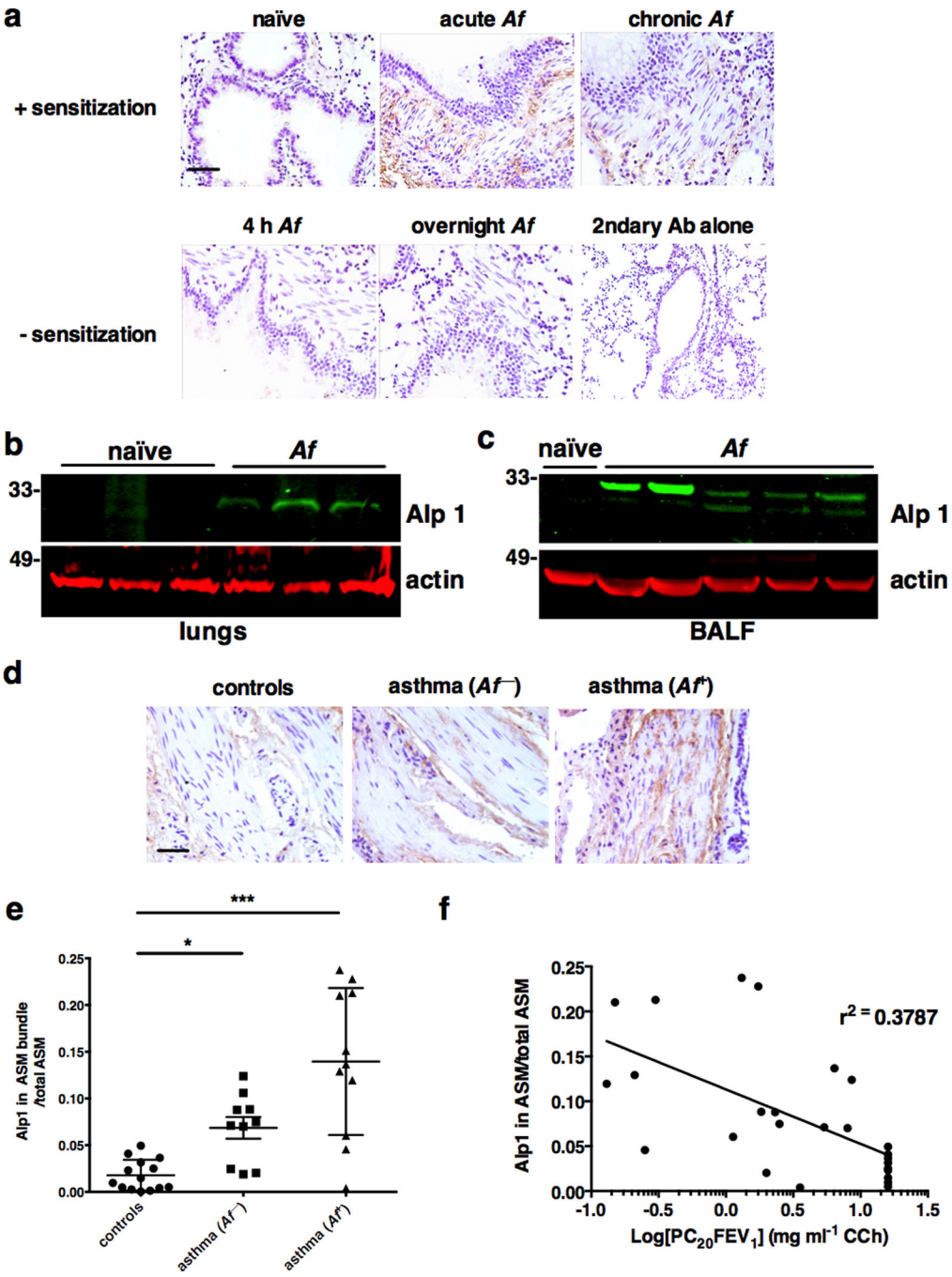

Figure 8. Alp 1 is detectable in the bronchial submucosa

(**a**) Top panel: BALB/c mice were sensitized intraperitoneally with *Af* crude extract (20 μg) mixed with 20 mg Alum on days 0 and 14. Mice were challenged intranasally with PBS ("naïve") or *Af* extract (25 μg, "acute") on days 25, 26 and 27, or challenged intranasally with *Af* extract without prior sensitization (50 μg on days 0, 7 and 14 and then with 20 μg twice per week for 4 weeks) ("chronic"). All mice were sacrificed 24 hours after the last challenge. Bottom panel: Naïve mice were challenged intranasally with *Af* extract (25 μg) and sacrificed after four hours or overnight. Alp 1 was detected using specific antisera and

DAB staining of paraffin-fixed lung sections. Sections were counterstained with hematoxylin. Images are representative of four to five mice per group (Scale bar, 50 μm; original magnification, 40x). (**b-c**) Alp 1 was detected in lysates of whole lung tissue (b) or BAL fluid (c) by immunoblotting. (**d**) Lung sections from healthy controls and subjects with asthma [with (Af^+) and without (Af^-) *Af* sensitivity] were immunostained with anti-Alp 1 antisera as above. Images are representative of 10-14 subjects/group (Scale bar, 50 μm; original magnification, 40x). (**e**) Alp 1 staining in the smooth muscle bundle was quantified using Image-pro Plus software and represented as the Alp 1^+ ASM/total ASM area (*P = 0.034, *** P = 0.0001, Kruskal Wallis). (**f**) Correlation between the PC_{20}FEV1 and Alp 1 staining for each subject.

Table 1

Clinical characteristics of patients studied

	Controls	Asthma-no *Af* sensitivity	Asthma +*Af* sensitivity
Number	14	10	12
Age*	28 (2.8)	29 (2.7)	41 (4.4)
Male/Female	5/9	6/4	6/6
$PC_{20}FEV_1$#	≥30 (33–219)	3.6 (1.8–8.6)**	0.67 (0.25–1.8)
Pre-BD FEV_1 (%predicted)‡	101.5 (97–106)	90.4 (71–115)	85.1 (64–126)
Inhaled corticosteroids†	None	5(400)	5(600)
LABA††	None	3(83)	3(83)
Positive *Af* skin test	0	0	12

*mean (± s.e.m.)

#geometric mean (95% CI)

**$P = 0.01$, Mann-Whitney *t* test *vAf* sensitive group

‡mean (range)

†number of subjects (equivalent of fluticasone propionate, μg)

††number of subjects (equivalent of salmeterol, μg). Control group FEV_1 and PC_{20} values do not include five patients in whom data were not available.